

# Distribution and Evolution of Fukushima Dai-ichi derived $^{137}\text{Cs}$ , $^{90}\text{Sr}$ , and $^{129}\text{I}$ in Surface Seawater off the Coast of Japan

Jennifer A. Kenyon,\* Ken O. Buesseler, Núria Casacuberta, Maxi Castrillejo, Shigeyoshi Otsuka, Pere Masqué, Jessica A. Drysdale, Steven M. Pike, and Virginie Sanial



Cite This: *Environ. Sci. Technol.* 2020, 54, 15066–15075



Read Online

ACCESS |



Metrics & More

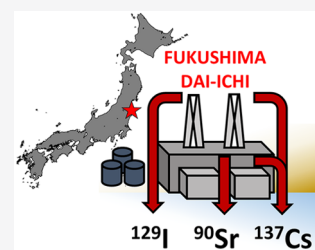


Article Recommendations



Supporting Information

**ABSTRACT:** The Fukushima Dai-ichi Nuclear Power Plants (FDNPPs) accident in 2011 led to an unprecedented release of radionuclides into the environment. Particularly important are  $^{90}\text{Sr}$  and  $^{137}\text{Cs}$  due to their known health detriments and long half-lives ( $T_{1/2} \approx 30$  y) relative to ecological systems. These radionuclides can be combined with the longer-lived  $^{129}\text{I}$  ( $T_{1/2} = 15.7$  My) to trace hydrologic, atmospheric, oceanic, and geochemical processes. This study seeks to evaluate  $^{137}\text{Cs}$ ,  $^{90}\text{Sr}$ , and  $^{129}\text{I}$  concentrations in seawater off the coast of Japan, reconcile the sources of contaminated waters, and assess the application of  $^{137}\text{Cs}/^{90}\text{Sr}$ ,  $^{129}\text{I}/^{137}\text{Cs}$ , and  $^{129}\text{I}/^{90}\text{Sr}$  as oceanic tracers. We present new data from October 2015 and November 2016 off the coast of Japan, with observed concentrations reaching up to  $198 \pm 4$  Bq·m $^{-3}$  for  $^{137}\text{Cs}$ ,  $9.1 \pm 0.7$  Bq·m $^{-3}$  for  $^{90}\text{Sr}$ , and  $(114 \pm 2) \times 10^{-5}$  Bq·m $^{-3}$  for  $^{129}\text{I}$ . The utilization of activity ratios suggests a variety of sources, including sporadic and independent releases of radiocontaminants. Though overall concentrations are decreasing, concentrations are still elevated compared to pre-accident levels. In addition, Japan's Environment Minister has suggested that stored water from the FDNPPs may be released into the environment and thus continued efforts to understand the fate and distribution of these radionuclides is warranted.



## 1. INTRODUCTION

The Fukushima Dai-ichi Nuclear Power Plants (FDNPPs) accident was the largest nuclear disaster since Chernobyl<sup>1</sup> and the greatest uncontrolled direct release of artificial radionuclides into the ocean,<sup>2</sup> with contaminated waters containing  $^{137}\text{Cs}$  ( $T_{1/2} = 30.2$  y),  $^{90}\text{Sr}$  ( $T_{1/2} = 28.9$  y), and  $^{129}\text{I}$  ( $T_{1/2} = 15.7$  My), among many other anthropogenic radionuclides (e.g.,  $^{134}\text{Cs}$ ,  $^{131}\text{I}$ ,  $^3\text{H}$ , etc.). Five primary pathways have been identified that allowed for the release of artificial radionuclides into the environment as a consequence of the events triggered by the Tohoku earthquake in March 2011: (i) direct deposition of radionuclides to the land and ocean via atmospheric fallout, (ii) direct discharge of spent reactor cooling fluid into the surrounding waters, (iii) localized discharges from the surrounding areas of the FDNPPs, (iv) transportation from land via river runoff, and (v) redissolution from beach sands as a result of submarine groundwater discharge.<sup>3,4</sup>

Although the ocean has a large capacity to disperse and dilute radioactive contamination, long-lived radionuclides can persist in the marine environment on time scales long enough to affect the marine ecosystem and, in turn, human health through the marine food chain.<sup>5</sup> The release of these radionuclides, although undesirable, allows for the unexpected opportunity to better understand ocean dynamics through the use of FDNPPs-derived radionuclides as tracers in the North Pacific Ocean. This study focuses on  $^{137}\text{Cs}$ ,  $^{90}\text{Sr}$ , and  $^{129}\text{I}$  concentrations and ratios due to their long half-lives, large

volumes of release, and ability to be reliably measured. Previously, ratios such as  $^{134}\text{Cs}/^{137}\text{Cs}$  were utilized following the accident, but  $^{134}\text{Cs}$  ( $T_{1/2} = 2.06$  y) will soon reach undetectable values in most of the Pacific Ocean due to decay and dilution.<sup>3</sup> For this reason, the utilization of ratios of isotopes with longer half-lives, such as  $^{90}\text{Sr}$  or  $^{129}\text{I}$ , is necessary.

**1.1. Pre- and Post-FDNPPs Accident Concentrations of  $^{137}\text{Cs}$ ,  $^{90}\text{Sr}$ , and  $^{129}\text{I}$ .** The presence of artificial radionuclides in the Pacific Ocean is governed by signals directly sourced from the FDNPPs accident, as well as by global fallout from atmospheric nuclear weapons testing that peaked in the 1950s and 1960s. Pre-FDNPPs accident average background concentrations in surface seawater are estimated to be 1–2 Bq·m $^{-3}$  for  $^{137}\text{Cs}$ ,<sup>6</sup>  $\sim 1$  Bq·m $^{-3}$  for  $^{90}\text{Sr}$ ,<sup>7,8</sup> and  $(1-2) \times 10^{-5}$  Bq·m $^{-3}$  for  $^{129}\text{I}$ .<sup>9,10</sup> Following the FDNPPs accident, significant attention has been given to understanding the distribution of FDNPPs-derived  $^{137}\text{Cs}$  concentrations. The majority of  $^{137}\text{Cs}$  released in the weeks after the accident was due to atmospheric and liquid discharges, with estimates of the total amount of  $^{137}\text{Cs}$  released to the environment ranging from 19–24 PBq.<sup>3</sup> This resulted in an increase of 22–27% from the pre-FDNPPs

Received: August 7, 2020

Revised: October 23, 2020

Accepted: October 26, 2020

Published: November 10, 2020



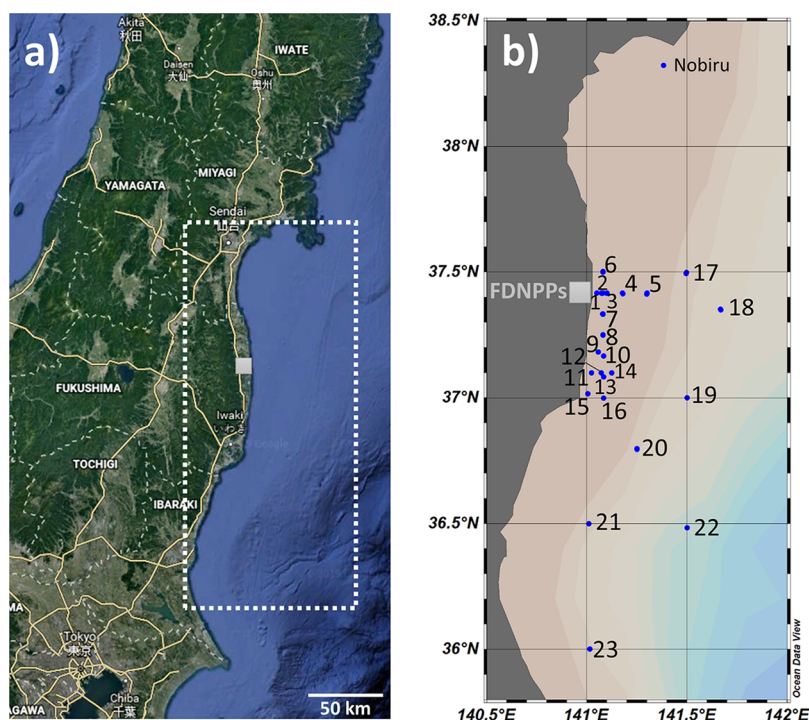


**Figure 1.** (a) Map off the coast of Japan indicating the sampling area (dashed white box). (b) Sampling stations from cruises in October 2015 (R/V Shinsei Maru) and November 2016 (R/V Shinsei Maru). The Fukushima Dai-Ichi Nuclear Power Plants are indicated by a gray box.

$^{137}\text{Cs}$  inventory in the North Pacific Ocean.<sup>3,11</sup> Liquid discharges peaked 3 weeks after the accident, with concentrations of  $^{137}\text{Cs}$  in seawater near the FDNPPs discharge channels reaching  $68 \times 10^6 \text{ Bq}\cdot\text{m}^{-3}$  on 6 April 2011.<sup>2</sup>

The monitoring of  $^{90}\text{Sr}$  has been given significantly less attention, due to comparatively more complicated methods for its radiochemical analysis and lower total release compared to other radionuclides such as Cs. The primary release pathway for  $^{90}\text{Sr}$  was direct FDNPPs liquid discharge of contaminated cooling water to the ocean, with estimates of total releases ranging from 0.04 to 1.0 PBq.<sup>12,13</sup> Measurements of  $^{90}\text{Sr}$  FDNPPs fallout levels on land were up to 3 orders of magnitude lower than those of  $^{137}\text{Cs}$ , primarily due to the lower volatility of  $^{90}\text{Sr}$ . An additional difference is that  $^{90}\text{Sr}$  is less likely to be accumulated in soil than Cs,<sup>3,14</sup> and is largely soluble in both freshwater and seawater conditions. Seawater concentrations measured shortly after the accident showed  $^{90}\text{Sr}$  levels up to eighty-five times higher than background levels.<sup>12,15</sup> Although  $^{90}\text{Sr}$  levels have been decreasing since the accident,  $^{90}\text{Sr}$  concentrations continue to be above pre-accident levels and detectable unintended releases occurring after the initial accident have been observed.<sup>16</sup>

$^{129}\text{I}$  has been less well studied than  $^{137}\text{Cs}$  and  $^{90}\text{Sr}$  due to its relatively long half-life and low oceanic inventory (and hence difficulty to measure). It is estimated that 0.2 TBq of  $^{129}\text{I}$  were released as a result of the FDNPPs accident with continued observations of  $^{129}\text{I}$  above pre-accident levels in the years following the accident.<sup>17–19</sup> The primary sources of  $^{129}\text{I}$  to the environment are a result of nuclear weapons testing and the reprocessing of spent nuclear fuel, principally in France and the United Kingdom.<sup>20</sup> Like Cs, I is volatile under the conditions of the accident at the FDNPPs in 2011 and would have been released both to the atmosphere and as liquid discharges. Because of its high solubility, long half-life, and prominent anthropogenic signal,  $^{129}\text{I}$  has been used as an oceanographic

transient tracer to study contemporary local to basin-scale circulation dynamics.<sup>9,21</sup>

**1.2. Activity Ratios to Constrain Sources of Fukushima-Derived Radionuclides.** Activity ratios, such as  $^{137}\text{Cs}/^{134}\text{Cs}$ ,  $^{137}\text{Cs}/^{90}\text{Sr}$ , and  $^{131}\text{I}/^{137}\text{Cs}$ , have been used extensively in prior studies to determine the sources of  $^{137}\text{Cs}$  and  $^{90}\text{Sr}$  to the marine environment.<sup>2,9,14,16,17,22</sup> This is possible because each source is characterized by distinct radionuclide ratios which result in measured ratios in the ocean that can be used to quantify their sources. The two primary sources of  $^{137}\text{Cs}$ ,  $^{90}\text{Sr}$ , and  $^{129}\text{I}$  labeling the waters off the coast of Japan include global fallout from nuclear weapons testing (e.g.,  $^{137}\text{Cs}/^{90}\text{Sr} \approx 1.6$ ,  $^{129}\text{I}/^{90}\text{Sr} \approx 2.3 \times 10^{-5}$ , and  $^{129}\text{I}/^{137}\text{Cs} \approx 7 \times 10^{-6}$ ), and releases from the FDNPPs accident.<sup>9,12</sup> While activity ratios from global fallout remain relatively constant in space and time, ratios of direct releases from the FDNPPs accident have varied. This can therefore be used as a means of understanding the specific sources within the FDNPPs: while initial atmospheric releases had a  $^{137}\text{Cs}/^{90}\text{Sr}$  ratio of  $\sim 1000$  in March 2011, secondary releases in the form of liquid discharges to the sea had a lower  $^{137}\text{Cs}/^{90}\text{Sr}$  ratio of  $39 \pm 1$  and a  $^{129}\text{I}/^{137}\text{Cs}$  ratio of  $4.1 \times 10^{-7}$ , decay corrected to the 6 April 2011 liquid discharge peak.<sup>3,9,12</sup> Since then, the ratios have varied greatly from the immediate post-accident ratio,<sup>12</sup> either because decontamination activities showed better performance for some radionuclides compared to others or because the specific sources of contamination and release processes from the FDNPPs were labeled by different radionuclide ratios (i.e., atmospheric release, wastewater, and groundwater discharge).

This study's primary objectives are to constrain the sources and temporal evolution of FDNPPs-derived  $^{137}\text{Cs}$ ,  $^{90}\text{Sr}$ , and  $^{129}\text{I}$  as well as assess the viability of FDNPPs-derived activity ratios as oceanographic tracers. We do so by examining the temporal evolution and the spatial distributions of  $^{137}\text{Cs}$ ,  $^{90}\text{Sr}$ ,

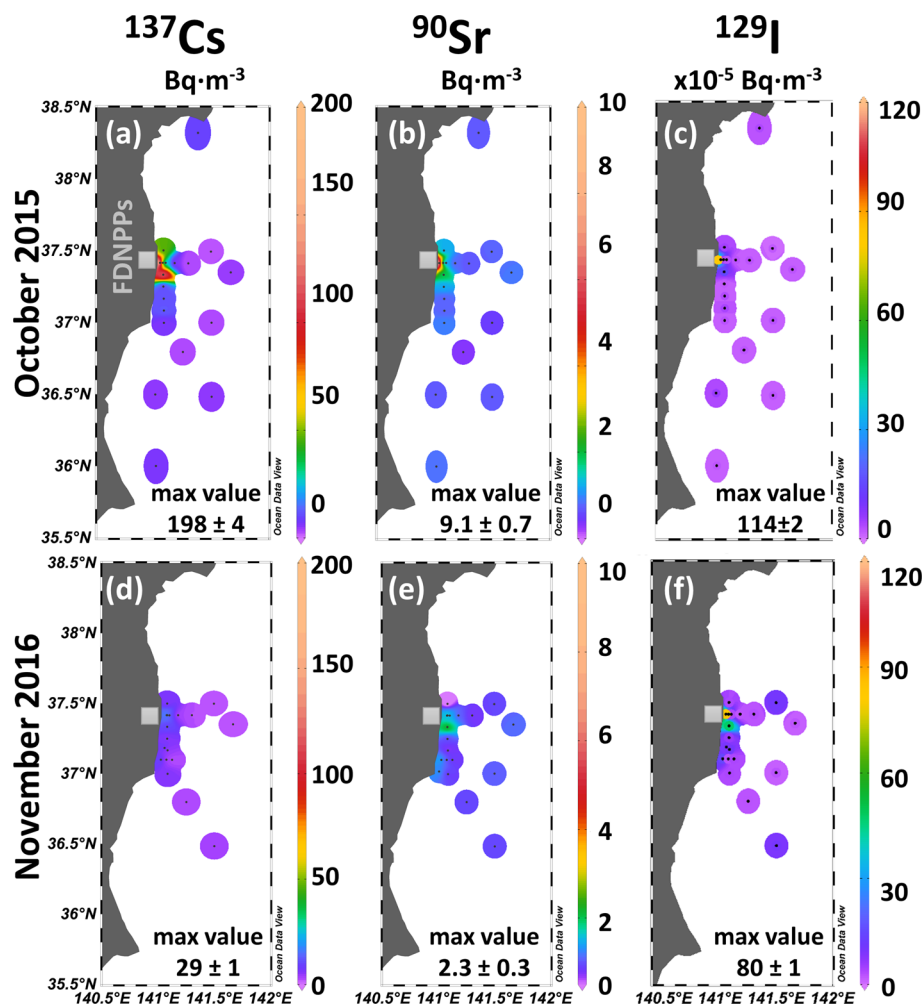


**Figure 2.** Concentrations of  $^{137}\text{Cs}$  (a,d),  $^{90}\text{Sr}$  (b,e), and  $^{129}\text{I}$  (c,f) in surface waters in October 2015 (upper plots) and November 2016 (lower plots). Pre-FDNPPs concentrations from literature (decay corrected to time of sampling) are  $1\text{--}2\text{ Bq}\cdot\text{m}^{-3}$  for  $^{137}\text{Cs}$ ,<sup>6</sup>  $\sim 1\text{ Bq}\cdot\text{m}^{-3}$  for  $^{90}\text{Sr}$ ,<sup>7,8</sup> and  $1\text{--}2 \times 10^{-5}\text{ Bq}\cdot\text{m}^{-3}$  for  $^{129}\text{I}$ .<sup>9,10</sup> Note the difference in scales. Highest concentrations are indicated. The location of the FDNPPs is indicated by a gray square. Plots generated using Ocean Data View.<sup>31</sup>

and  $^{129}\text{I}$  since the FDNPPs accident in seawater considering previously published and new data from 2015 and 2016. This analysis includes identifying specific meteorological events and physical factors affecting radionuclide inputs into the ocean and assessing the effectiveness of the man-made decontamination systems. We use the  $^{137}\text{Cs}/^{90}\text{Sr}$ ,  $^{129}\text{I}/^{137}\text{Cs}$ , and  $^{129}\text{I}/^{90}\text{Sr}$  ratios to identify the different source terms (i.e., FDNPPs, weapons testing) of the specific radionuclides and utilize the evolution of the activity ratios to better understand release processes.

## 2. MATERIALS AND METHODS

**2.1. Study Area and Sample Collection.** New results are presented from surface seawater samples that were collected during two cruises off the coast of Japan in October 2015 and November 2016 (R/V Shinsei Maru). Sampling stations (Figure 1) were located between  $\sim 1$  to  $\sim 160$  km offshore of the FDNPPs. Sample collection consisted of on-board collection via the ship's flow-through system, off-board collection via surface pump, and collection via CTD rosette equipped with Niskin bottles. Our results will be discussed together with previously published data collected on cruises from June 2011 (R/V Ka'imikai-O-Kanaloa), September 2013

(R/V Daisan Kaiyo Maru), May 2014 (R/V Shinsei Maru), and October 2014 (R/V Shinsei Maru).<sup>9,12,16,23</sup> The cruises performed after 2012 revisited the same stations on an annual basis, therefore allowing for characterization of the time-evolution of radionuclide distribution in this specific domain (Figure 1b).

**2.2. Radiochemistry and Measurement of  $^{137}\text{Cs}$ ,  $^{90}\text{Sr}$ , and  $^{129}\text{I}$ .** Seawater samples for  $^{137}\text{Cs}$  and  $^{90}\text{Sr}$  were collected and stored in 20 L cubitainers. Before the initial chemical separation, Cs (0.5–0.7 mg) and Sr ( $\sim 200$  mg) stable carriers were added to the samples to determine extraction recovery via inductively coupled plasma mass spectrometer (Thermo iCAP Qc). Seawater samples were initially passed through a precolumn  $20\ \mu\text{m}$  frit. Cs was then extracted via absorption onto columns containing 5 mL of KNiFC-PAN ion absorber resin (Czech Technical University, Prague). The resin was then dried at low temperature ( $<60\ ^\circ\text{C}$ ) for  $\gamma$ -counting on high-purity germanium well detectors.<sup>24–26</sup> The minimum detectable activity (MDA) for  $^{137}\text{Cs}$  range was from  $0.1\text{--}0.2\text{ Bq}\cdot\text{m}^{-3}$  for average counting times of 50 h. Concentration uncertainties were calculated via propagation of uncertainties in count rate and detector calibrations. The extraction recovery for Cs was 91 to 99% across all samples, and the loss of Sr through the KNiFC-PAN resin was, on average,  $< 4\%$ .

$^{90}\text{Sr}$  activity was determined via isolation and measurement of its daughter product,  $^{90}\text{Y}$  ( $T_{1/2} = 64.1$  h). Upon Cs extraction, the 20 L water samples were left undisturbed for at least 28 days in order to re-establish secular equilibrium between  $^{90}\text{Sr}$  and  $^{90}\text{Y}$ . Prior to chemical extraction, samples were spiked with 10  $\mu\text{g}$  of a stable Y carrier. Samples prior to 2016 were analyzed using the procedure outlined in Casacuberta et al. (2013) via coprecipitation with iron hydroxides and purified using anion (Bio-Rad AGI-X8, 100–200 mesh) and cation (Bio-Rad AG50W-X8, 100–200 mesh) ion-exchange columns.<sup>27</sup> Samples analyzed in 2016 and onward were analyzed via an adapted method from Tazoe et al. (2016),<sup>28</sup> which reduced the presence of competing beta signals (refer to S1) by utilizing Eichrom DGA resin 1 mL cartridges. Postcolumn samples were filtered through a 25 mm QMA filter, dried, and fixed onto beta mounts that were counted for  $^{90}\text{Y}$  on Risø beta detectors (Risø National Lab; Roskilde, Denmark). Aliquots were taken before and after chemical isolation for stable Y to determine extraction recovery via iCAP QC, with Y recoveries ranging from 48% to 98%. The MDA ranged from 0.2–0.4  $\text{Bq}\cdot\text{m}^{-3}$  for an approximate average 90 h counting time.

$^{129}\text{I}$  seawater samples were collected and stored in 0.4 L amber bottles until processing. Seawater samples ranging from 0.2–0.4 L were spiked with a Woodward stable iodine carrier (1–1.5 mg of  $^{127}\text{I}$ ). All iodine species in the samples were first oxidized to iodate using  $\text{Ca}(\text{ClO})_2$  and subsequently transformed to iodide using 1 M  $[\text{NH}_2\text{OH}]\cdot\text{HCl}$  together with  $\text{Na}_2\text{O}_5\text{S}_3$ . Thus, all iodine species are in iodide form before purification with BioRad 1  $\times$  8 analytical grade resins and precipitation as AgI using a solution of  $\text{AgNO}_3$ . The  $^{129}\text{I}/^{127}\text{I}$  ratio was determined for each sample using the ETH Zurich 0.5 MV AMS system Tandy, which allowed for the estimation of final  $^{129}\text{I}$  concentrations. The measured  $^{129}\text{I}/^{127}\text{I}$  ratios were normalized to the ETH Zurich in-house standard D22 with a nominal ratio  $^{129}\text{I}/^{127}\text{I}$  of  $(50.35 \pm 0.16) \times 10^{-12}$ .<sup>29</sup> Final concentrations of  $^{129}\text{I}$  were calculated from the blank corrected  $^{129}\text{I}/^{127}\text{I}$  ratios and the known amount of  $^{127}\text{I}$  carrier.<sup>30</sup> More information on all radiochemical analyses can be found in S1.

### 3. RESULTS

At the time of sampling, surface concentrations of  $^{137}\text{Cs}$  ranged from  $2.1 \pm 0.1$  to  $198 \pm 4$   $\text{Bq}\cdot\text{m}^{-3}$  in 2015 and  $2.0 \pm 0.1$  to  $29.0 \pm 0.7$   $\text{Bq}\cdot\text{m}^{-3}$  in 2016 (Figure 2a,d). Results of  $^{90}\text{Sr}$  ranged from  $0.3 \pm 0.2$  to  $9.1 \pm 0.7$   $\text{Bq}\cdot\text{m}^{-3}$  in 2015 and from  $0.6 \pm 0.1$  to  $2.3 \pm 0.2$   $\text{Bq}\cdot\text{m}^{-3}$  in 2016 (Figure 2b,e). Surface  $^{129}\text{I}$  ranged from  $(1.52 \pm 0.06) \times 10^{-5}$  to  $(114 \pm 2) \times 10^{-5}$   $\text{Bq}\cdot\text{m}^{-3}$  in 2015 and  $(1.9 \pm 0.2) \times 10^{-5}$  to  $(80 \pm 1) \times 10^{-5}$   $\text{Bq}\cdot\text{m}^{-3}$  in 2016 (Figure 2c,f). Highest concentrations were always observed at station 1, the station nearest ( $\sim 1.6$  km) the FDNPPs. A full list of results can be found in S3.

We calculated the  $^{137}\text{Cs}/^{90}\text{Sr}$ ,  $^{129}\text{I}/^{137}\text{Cs}$ , and  $^{129}\text{I}/^{90}\text{Sr}$  activity ratios using data obtained in 2015 and 2016 (Figures 3 and 4c) to provide insight into the sources of artificial radionuclides off the coast of Japan. The  $^{137}\text{Cs}/^{90}\text{Sr}$  ratio shifted from  $104 \pm 6$  in October 2015 (dominated by an event on 10 October 2015, described later) to  $16.0 \pm 0.4$  in November 2016 for surface samples less than 10 km from the FDNPPs (Figure 3). The  $^{129}\text{I}/^{137}\text{Cs}$  and  $^{129}\text{I}/^{90}\text{Sr}$  ratios within 10 km of the FDNPPs also varied greatly from 2015 to 2016. The  $^{129}\text{I}/^{137}\text{Cs}$  ratio increased from  $(0.090 \pm 0.001) \times 10^{-5}$  to  $(1.9 \pm 0.2) \times 10^{-5}$ , and the  $^{129}\text{I}/^{90}\text{Sr}$  ratio similarly increased

from  $(9 \pm 1) \times 10^{-5}$  to  $(36 \pm 7) \times 10^{-5}$ . There exists an outlier sample in the 2015 data, which has a  $^{137}\text{Cs}/^{90}\text{Sr}$  ratio of  $5.4 \pm 0.2$ ,  $^{129}\text{I}/^{137}\text{Cs}$  ratio of  $(2.3 \pm 0.5) \times 10^{-5}$  and  $^{129}\text{I}/^{90}\text{Sr}$  ratio of  $(12.5 \pm 0.7) \times 10^{-5}$ .

## 4. DISCUSSION

**4.1. Constraining Sources of  $^{137}\text{Cs}$ ,  $^{90}\text{Sr}$ , and  $^{129}\text{I}$  off the Coast of Japan in 2015 and 2016.** In samples collected over 10 km away from the FDNPPs (not included in the linear regressions in Figure 3), activity ratios are comparable to pre-accident levels and are likely dominated by waters that originate from the open ocean and have not come into contact with the FDNPPs site. Samples near the FDNPPs exhibiting a very low  $^{137}\text{Cs}/^{90}\text{Sr}$  ratio would be indicators of  $^{90}\text{Sr}$  accidental releases similar to those that occurred in December 2011 and March 2012,<sup>15,16</sup> denoted in Figure 4c; however, similar observations were not seen in data from October 2015 and November 2016. It is likely that the sporadic change over time is due to variable and independent releases of both  $^{137}\text{Cs}$  and  $^{90}\text{Sr}$  from the reactor facilities, with large variations in  $^{137}\text{Cs}$  dominating the observed ratio (as shown in Figures 3 and 4). This is partly caused by the distinct efficiencies in the removal of different radionuclides via various decontamination systems (see Section 4.4).

The  $^{129}\text{I}/^{137}\text{Cs}$  ratio (Figure 3c) immediately after the accident as measured in seawater was  $4.1 \times 10^{-7}$ : a sharp decrease from the pre-accident ratio of  $7 \times 10^{-6}$  that can be explained by the large amount of  $^{137}\text{Cs}$  released relative to  $^{129}\text{I}$ .<sup>9</sup> A previous study by Casacuberta et al. reported that the  $^{129}\text{I}/^{137}\text{Cs}$  ratios in seawater may decrease over time due to the higher particle scavenging efficiency of  $^{137}\text{Cs}$  compared to  $^{129}\text{I}$ , although it was noted in this study that the distribution coefficients for  $^{137}\text{Cs}$  ( $K_d = 2000$  L/kg) and  $^{129}\text{I}$  ( $K_d = 70$  L/kg) are both relatively low and that scavenging may have little or no measurable impact compared to transport by water currents over time scales of several years.<sup>23</sup> On the basis of the high variability of average  $^{129}\text{I}/^{137}\text{Cs}$  ratios between sampling times, preferential Cs scavenging is likely not an explanation for the changing  $^{129}\text{I}/^{137}\text{Cs}$  ratios. Indeed, it has been found that coastal sediments near the FDNPPs selectively release  $^{129}\text{I}$  over  $^{137}\text{Cs}$ .<sup>32</sup> The most likely explanation is ongoing variable releases of  $^{129}\text{I}$  while  $^{137}\text{Cs}$  is more effectively being removed via radionuclide decontamination systems at the FDNPPs, thereby leading to an increase in the  $^{129}\text{I}/^{137}\text{Cs}$  ratio. The  $^{129}\text{I}/^{90}\text{Sr}$  ratios (Figure 3d) were similarly higher in 2016 ( $36 \pm 7 \times 10^{-5}$ ) than 2015 ( $9 \pm 1 \times 10^{-5}$ ). This gives credence to the notion that  $^{129}\text{I}$  is released sporadically and independently of other radionuclides such as  $^{90}\text{Sr}$ , which is sourced from the FDNPPs site and at least partially removed via decontamination systems (further discussed in Section 4.4 and S2).

Uniquely interesting are the near-shore samples collected on 10 October 2015 (Figure 3, blue triangles), since their radionuclide levels, particularly  $^{137}\text{Cs}$  ( $46$ – $198$   $\text{Bq}\cdot\text{m}^{-3}$ ), are elevated. Samples from this date dominate the higher components of the  $^{137}\text{Cs}/^{90}\text{Sr}$  ratio (Figure 3a) and correspondingly lower  $^{129}\text{I}/^{137}\text{Cs}$  and  $^{129}\text{I}/^{90}\text{Sr}$  ratios. If these samples were directly affected from releases from the FDNPPs, one would expect a lower  $^{137}\text{Cs}/^{90}\text{Sr}$  ratio and a higher  $^{129}\text{I}/^{137}\text{Cs}$  ratio. The samples that exhibited the elevated contamination were from stations 1, 6, and 7, which are the stations closest to the shore. As discussed by Sanial et al. (2017), high  $^{137}\text{Cs}$  concentrations are found in sands and

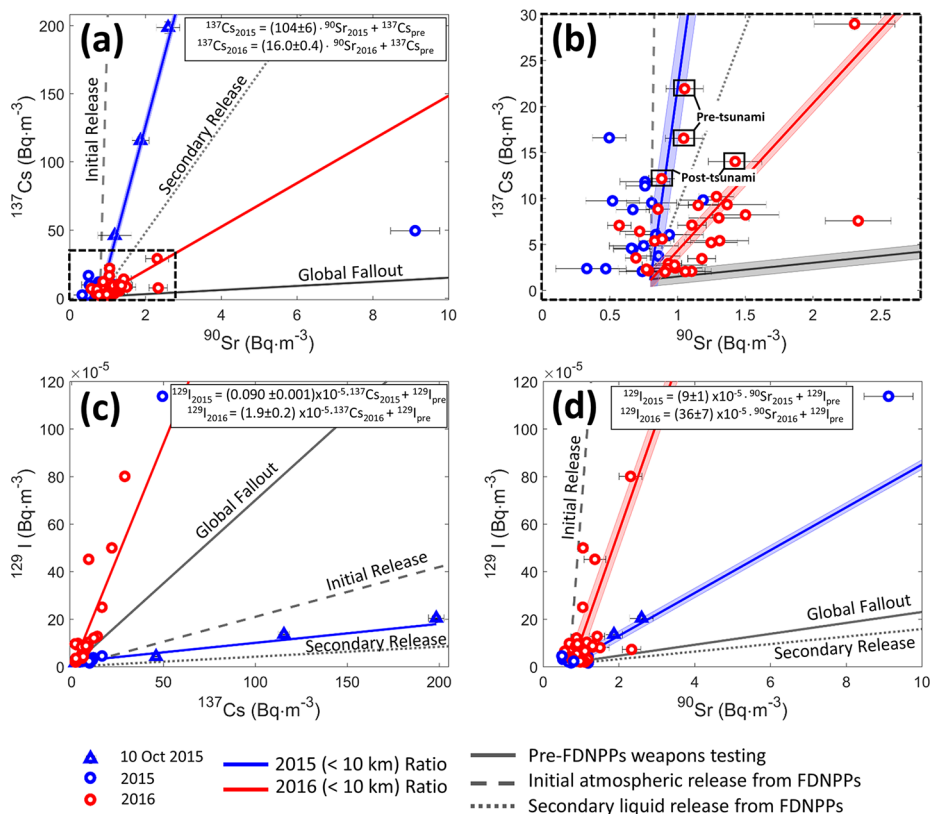


**Figure 3.** (a)  $^{137}\text{Cs}$  vs  $^{90}\text{Sr}$  concentrations in surface seawater from 2015 (blue) and 2016 (red) cruises. (b) Inset of part a with focus on lower values ( $^{137}\text{Cs} < 30 \text{ Bq}\cdot\text{m}^{-3}$  and  $^{90}\text{Sr} < 3 \text{ Bq}\cdot\text{m}^{-3}$ ). (c)  $^{129}\text{I}$  vs  $^{137}\text{Cs}$  and (d)  $^{129}\text{I}$  vs  $^{90}\text{Sr}$  from 2015 (blue), and 2016 (red). Linear regressions for 2015 and 2016 surface seawater samples within 10 km of the FDNPPs are shown on the plots. Solid gray line represents pre-FDNPPs accident background ratios as a result of weapons testing (using values of  $2 \text{ Bq}\cdot\text{m}^{-3}$  for  $^{137}\text{Cs}$ ,  $1 \text{ Bq}\cdot\text{m}^{-3}$  for  $^{90}\text{Sr}$ , and  $2 \times 10^{-5} \text{ Bq}\cdot\text{m}^{-3}$  for  $^{129}\text{I}$ ). Dashed gray line represents the ratio of the initial atmospheric release from the FDNPPs accident (e.g., March 2011). Dotted gray line indicates the ratio at the peak of the liquid release from the FDNPPs accident (e.g., April 2011). Shaded bars represent uncertainty.

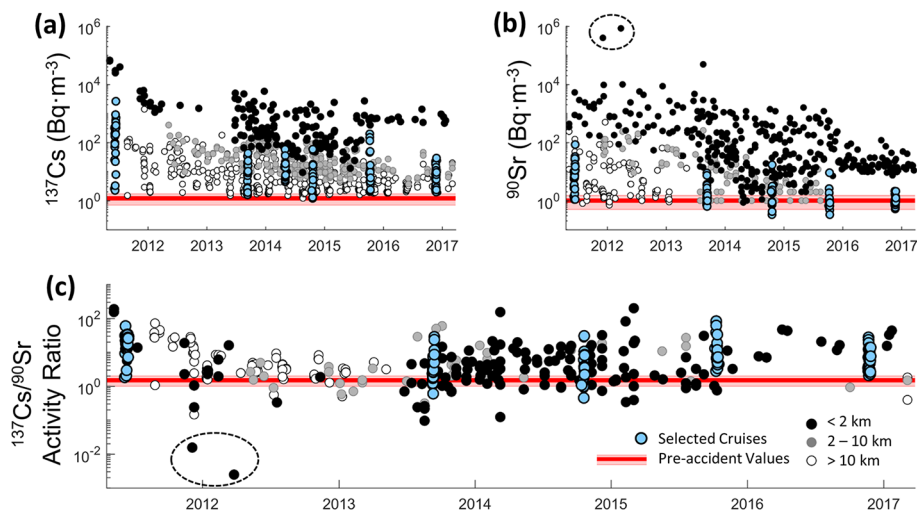


**Figure 4.** Time series analysis of  $^{137}\text{Cs}$  and  $^{90}\text{Sr}$  in surface seawater from publicly available data from the Japanese Atomic Energy Agency (black, gray, and white circles for  $< 2 \text{ km}$ ,  $2\text{--}10 \text{ km}$ , and  $> 10 \text{ km}$ , respectively) and from selected cruises (blue circles, detailed in Section 2.1).<sup>9,12,16,23,30</sup> Points within the dotted black ellipses represent previously acknowledged accidental releases.<sup>16</sup> Red lines indicate pre-accident values (i.e., weapons testing derived values) with a shaded bar representing uncertainty.

sediments on beaches as far away as 56 km from the reactor, which can subsequently be carried by along-shore coastal currents.<sup>33</sup> Alternatively, sandy sediments tend to selectively release  $^{129}\text{I}$  over  $^{137}\text{Cs}$  and thus have lower  $^{129}\text{I}$  concentrations as iodine binds to organic matter in the soil and is removed

from seawater.<sup>32,34</sup> This would result in a lower  $^{129}\text{I}/^{137}\text{Cs}$  ratio compared to the direct liquid discharges from the power plant.

There also exists an anomalous sample from 2015, which has much higher levels of  $^{90}\text{Sr}$  ( $9.1 \pm 0.7 \text{ Bq}\cdot\text{m}^{-3}$ ) and  $^{129}\text{I}$  ( $114 \pm 2 \times 10^{-5} \text{ Bq}\cdot\text{m}^{-3}$ ) as compared to the rest of the data from

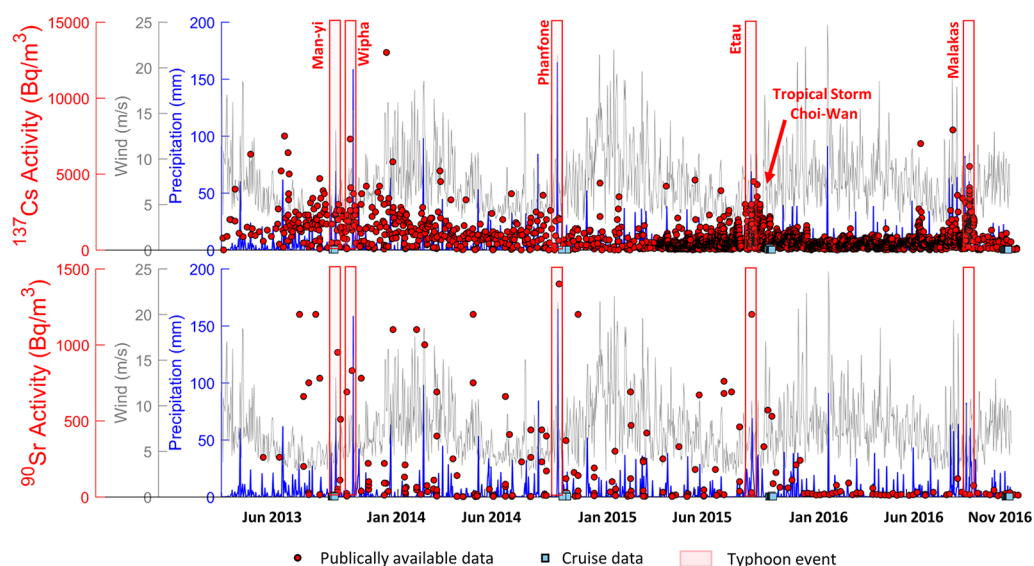


**Figure 5.** Surface seawater concentrations from publically available data<sup>15</sup> (red circles) and select cruises<sup>12,16</sup> (blue squares) of  $^{137}\text{Cs}$  (top panel) and  $^{90}\text{Sr}$  (bottom panel) within 1.5 km of the FDNPPs plotted with wind speed ( $\text{m}\cdot\text{s}^{-1}$ ) 10 m above the ground and average daily precipitation (mm) at Station Namie<sup>38</sup> in the Fukushima Prefecture, Japan. Typhoon events highlighted in red are as follows: Man-yi (Sept 2013), Wipha (Oct 2013), Phanfone (Oct 2014), Etai (Sept 2015, a severe tropical storm), Choi-Wan (Oct 2015, a localized tropical storm), and Malakas (Sept 2016).

2015 and 2016. This sample, taken closest to the reactor at station 1, suggests that elevated levels of radionuclides were still leaking directly from the FDNPPs area into the environment in 2015. It is important to note that the activity ratios can vary within a very short time span, as is the case here with variations within days or hours. Small scale variability due to coastal currents and tides will undoubtedly add to variability in radionuclide ratios that cannot be resolved with existing sampling resolution.

**4.2. Spatial and Temporal Distribution of  $^{137}\text{Cs}$ ,  $^{90}\text{Sr}$ , and  $^{129}\text{I}$  off the Coast of Japan (2011–2017).**  $^{137}\text{Cs}$  and  $^{90}\text{Sr}$  concentrations in surface water samples collected during several cruises off the coast of Japan in June 2011, September 2013, and October 2014 showed elevated concentrations of radionuclides in surface seawater near the FDNPPs (Figure 4, blue circles), with concentrations decreasing with distance from the FDNPPs.<sup>12,16</sup> Results for  $^{137}\text{Cs}$  and  $^{90}\text{Sr}$  from cruises in 2015 and 2016 show a similar spatial pattern (Figure 2), with maximum observed values far lower than values observed immediately following the accident. In addition to the annual data taken from cruises off the coast of Japan, the Japan Atomic Energy Agency (JAEA) has regularly compiled and publicly reported monitoring data from a variety of agencies, notably the Tokyo Electric and Power Company (TEPCO) and the Fukushima Prefecture, for  $^{137}\text{Cs}$  and  $^{90}\text{Sr}$  in surface waters surrounding the FDNPPs since the accident. Waters less than 2 km away from the FDNPPs show higher than pre-accident levels by an order of magnitude through 2017. Persistently elevated concentrations indicate ongoing releases from the FDNPPs at the time of this study's sampling of surface seawater. It is worth noting that the concentrations recorded are higher than those predicted by model simulations that consider advection and mixing and assume no substantial releases of radionuclides post-FDNPPs disaster.<sup>35,36</sup> More than 2 km away from the FDNPPs, values for  $^{137}\text{Cs}$  and  $^{90}\text{Sr}$  more closely resemble pre-accident levels, likely indicating that such releases are diluted due to offshore water transport.

There has been a reduction in the spatial and temporal monitoring of  $^{137}\text{Cs}$  and  $^{90}\text{Sr}$  monitoring over time, particularly toward the end of 2015 with continued monitoring focusing on the area directly adjacent to the power plant. In addition to a reduced frequency in observation, JAEA data has limited information on sample uncertainties as well as variable minimum detectable activities (MDAs), some of which are higher than pre-accident concentrations. For example, the average MDA for TEPCO, which supplies monitoring data to JAEA, was up to the order of  $10^4 \text{ Bq}\cdot\text{m}^{-3}$  for  $^{137}\text{Cs}$  for the first couple of months after the accident: 3 orders of magnitude higher than pre-FDNPPs levels. MDAs for TEPCO continued to be up to the order of  $10^3 \text{ Bq}\cdot\text{m}^{-3}$  for years after the accident. While certainly MDAs are high due to low volume sampling and short counting times in order to run as many samples as possible immediately after the accident, this leads to certain bias in the interpretation of TEPCO data. Despite this, JAEA reported observations remain useful in the interpretation of the changing patterns of radionuclide releases from the FDNPPs.

$^{129}\text{I}$  was sampled during cruises in June 2011, September 2013, May 2014, October 2014, October 2015, and November 2016, with the highest levels observed during these cruises occurring at stations near the FDNPPs.<sup>9,23,37</sup> It is important to note that observed  $^{129}\text{I}$  concentrations immediately after the accident were only up to an order of magnitude above pre-accident concentrations.<sup>9</sup> Unlike  $^{137}\text{Cs}$  and  $^{90}\text{Sr}$ ,  $^{129}\text{I}$  is not actively monitored by the JAEA, thus precluding inclusion of  $^{129}\text{I}$  in Figure 4 and Figure 5.

**4.3. Impacts of Storms on the Distributions of  $^{137}\text{Cs}$ ,  $^{90}\text{Sr}$ , and  $^{129}\text{I}$ .** To determine factors that affect radionuclide surface concentrations, it is necessary to also consider wind, precipitation, and storm events, as they have the potential to increase transport of radionuclides from terrestrial or near-shore sources to the open ocean via runoff and mixing. To this end, within a local scale (e.g., 1.5 km) of the FDNPPs, we compare  $^{137}\text{Cs}$  and  $^{90}\text{Sr}$  concentrations in surface seawater with precipitation, wind, and typhoon events at Station Namie<sup>38</sup> in

**Table 1. Summary of  $^{137}\text{Cs}$ ,  $^{90}\text{Sr}$ , and  $^{129}\text{I}$  Contributions via Various Source Inputs Described in This Study and Their Corresponding Activity Ratios<sup>a</sup>**

Source	$^{137}\text{Cs}$ $\text{Bq}\cdot\text{m}^{-3}$	$^{90}\text{Sr}$ $\text{Bq}\cdot\text{m}^{-3}$	$^{129}\text{I}$ $\text{Bq}\cdot\text{m}^{-3}$	$^{137}\text{Cs}/^{90}\text{Sr}$ $\frac{\text{Bq}\cdot\text{m}^{-3}}{\text{Bq}\cdot\text{m}^{-3}}$	$^{129}\text{I}/^{137}\text{Cs}$ $\frac{\text{Bq}\cdot\text{m}^{-3}}{\text{Bq}\cdot\text{m}^{-3}}$	$^{129}\text{I}/^{90}\text{Sr}$ $\frac{\text{Bq}\cdot\text{m}^{-3}}{\text{Bq}\cdot\text{m}^{-3}}$
Weapon's Testing <sup>8,9,10,11,12,14</sup>	1–2	1	$1\text{--}2 \times 10^{-5}$	1.6	0.7	2.3
FDNPPs Atmospheric Fallout (03/11) <sup>3,11,14</sup>	$10^6$	$10^2\text{--}10^3$	$10^1$	1000	0.2	210
Post-accident Direct Releases (04/11) <sup>3,11,14</sup>	$10^4\text{--}10^5$	$10^3\text{--}10^4$	$10^2\text{--}10^3$	39	0.04	1.6
2012 Tank Leak <sup>18</sup>	↑	↑	--	↓	--	--
Direct FDNPPs Land Runoff <sup>2,3,39,40,41,37</sup>	↑	↑	■	↓	↓	↓
Groundwater Discharge <sup>3,4,32,42</sup>	↑	■	↑	↑	↑	↑
Decontamination Systems <sup>45</sup>	↓	↓	■	↓	↑	↑
Precipitation <sup>15,38</sup>	↑	■	--	--	--	--
2016 Tsunami	■	■	--	■	--	--

<sup>a</sup>The ■ symbol indicates no significant change between pre-event or system and post-event or system was observed. The symbols ↑ and ↓ indicate the increased or decreased supply, respectively, of radionuclides for each release mechanism or source in both concentrations and ratios. The -- line indicates missing or inconclusive data.

the Fukushima Prefecture for the time period between 2013 and 2016 (Figure 5). Elevated  $^{137}\text{Cs}$  concentrations show a significant ( $p$ -value  $<0.05$ ) trend with high wind and high precipitation, especially during typhoon events (Figure 5, top panel). The exception to this is Typhoon Phanfone in October 2014, although sampling of  $^{137}\text{Cs}$  was very infrequent during this time compared to other times and may be a less accurate reflection of  $^{137}\text{Cs}$  surface concentrations. As previously mentioned, high  $^{137}\text{Cs}$  concentrations ( $46\text{--}198 \text{ Bq}\cdot\text{m}^{-3}$ ) were observed in coastally derived turbid waters on 10 October 2015. A possible explanation for this is groundwater discharge and coastal mixing caused by tropical storm Choi-Wan, which passed over the coast of Japan just days before the 2015 cruise. It is further postulated that elevated Cs during this event is due to high runoff; as previously observed in river studies, Cs is desorbed from fine soil particles during high precipitation events.<sup>39–41</sup> Suspended particles carried from land are estimated to desorb a few to 40% of  $^{137}\text{Cs}$  in the suspension as salinity increases.<sup>42,43</sup> The ratio of  $^{129}\text{I}/^{137}\text{Cs}$  in suspended particles of rivers is lower than that of marine sediments and should be considered as another process for selectively supplying  $^{137}\text{Cs}$  to coastal seawater.<sup>32</sup>

Although there exist samples that show elevated  $^{90}\text{Sr}$  values during events of high wind or precipitation, there is not a significant relationship between high wind or precipitation with elevated  $^{90}\text{Sr}$  concentrations (Figure 5). Perhaps this is not surprising, as the amount of  $^{90}\text{Sr}$  deposited to land is small compared to  $^{137}\text{Cs}$ .<sup>3,12</sup> Increased mixing and groundwater movement influenced by high winds and high precipitation are hence not considered to be significant contributors to elevated  $^{90}\text{Sr}$  concentrations in 2015. However, overflow of catchment basins in storage units on the grounds of the FDNPPs containing  $^{90}\text{Sr}$  is thought to be one source of elevated activity during times of high precipitation,<sup>44</sup> though this is not observed in our larger data set.

The effects that specific events can have on the concentrations of the radionuclides in seawater can also be illustrated by the data obtained when sampling just before and after a 7.4 magnitude earthquake and a subsequent 1.4 m tsunami which occurred on 22 November 2016 with an epicenter offshore of the Fukushima Prefecture. Samples were taken at stations near the FDNPPs the day before, the day after, and 2 days following the earthquake (Figure 3b, black squares). No increases in radionuclide concentrations were observed as a result of this minor tsunami (see S3 for more specific information). This is a likely reflection of uncon-

taminated offshore waters diluting waters at station 1, rather than the potential of radionuclide release to the environment.

**4.4. Effectiveness of man-made decontamination systems.** The observed decrease in radionuclide concentrations over time cannot exclusively be explained by natural processes described above (i.e., radioactive decay, dilution, scavenging, absorption by organic compounds, etc.). The implementation of decontamination systems, mostly by the end of 2015 (described in S2), may explain discrepancies or unresolved patterns observed for these radionuclides. This is particularly relevant for  $^{90}\text{Sr}$  which, unlike  $^{137}\text{Cs}$  and  $^{129}\text{I}$ , is neither abundant on land nor in coastal sediments, as reflected in the  $^{137}\text{Cs}/^{90}\text{Sr}$  ratio being consistently above background ratios after fall 2015 (Figure 4c). Additionally,  $^{90}\text{Sr}$  concentrations more than 2 km away from the FDNPPs were similar to background levels by the end of 2015, unlike  $^{137}\text{Cs}$  (Figure 4). However, decreased sampling regularity by the JAEA and affiliated government organizations makes it difficult to determine the effectiveness of these actions.<sup>44</sup> It is also difficult to infer the effectiveness of decontamination efforts on a cruise-to-cruise basis, as activity ratios vary greatly across cruises (Figures 3 and 4c).<sup>45</sup> Despite the introduction of these decontamination efforts, elevated radionuclide levels in surface waters off the coast of Japan were still observed by the end of 2016. In addition, Japan's Environment Minister has suggested that stored water from the FDNPPs may be released into the ocean in the future due to limitations in water storage capabilities.<sup>46,47</sup> For these reasons, this work and continued monitoring are important to understand the transport and fate of these radionuclides.

**4.5. Viability of Fukushima-Derived Activity Ratios as Oceanographic Tracers.** Estimates of the total amount of  $^{137}\text{Cs}$  released to the environment across multiple models converge around  $15\text{--}20 \text{ PBq}$  within the first few weeks of the accident, whereas total subsequent releases are estimated to be orders of magnitude lower.<sup>2</sup> This decreasing trend is similar for  $^{90}\text{Sr}$  and  $^{129}\text{I}$ .<sup>16,23</sup> Consequently, the vast majority of the FDNPPs signal in the Pacific Ocean will be dominated by activity ratios originating from the initial FDNPPs release, except very near the coast of Japan. Thus, only the initial  $^{137}\text{Cs}/^{90}\text{Sr}$  ratio of  $39 \pm 1$  is a reliable tracer for contaminated seawater into the greater Pacific Ocean. The  $^{129}\text{I}/^{137}\text{Cs}$  ratio was also thought to be a potentially viable tracer, with an initial seawater ratio of  $4.1 \times 10^{-7}$ .<sup>3,9</sup> However, the amount of  $^{129}\text{I}$  derived from the FDNPPs accident and later releases is only 2

orders of magnitude higher than the global fallout signal, making this FDNPPs pulse of  $^{129}\text{I}$  from 2011 very difficult to trace farther out into the Pacific Ocean. While the initial ratios dominate the signals of FDNPPs-derived radionuclides throughout the Pacific Ocean, those observed during subsequent and smaller releases (as summarized in Table 1) from the FDNPPs give insight into processes and sources occurring near the coast of Japan. In the case of this study, these ratios have already shown themselves useful in tracing sources and pathways of contaminated waters from the FDNPPs to the coast of Japan. These activity ratios will also be useful as a baseline in the event of deliberate releases of the >1 million tons of stored water on site, which itself has the potential to be a source of new tracers.<sup>46–48</sup>

## ■ ASSOCIATED CONTENT

### Supporting Information

The Supporting Information is available free of charge at <https://pubs.acs.org/doi/10.1021/acs.est.0c05321>.

S1, detailed information regarding radiochemical methods; S2, detailed information regarding decontamination efforts at the FDNPPs site; table S3, information regarding sampling date, locations, additional notes, and concentrations of  $^{137}\text{Cs}$ ,  $^{90}\text{Sr}$ , and  $^{129}\text{I}$  samples reported in this study ( $^{129}\text{I}$  samples are reported in  $\text{Bq}\cdot\text{m}^{-3}$  as well as  $\times 10^7 \text{ at}\cdot\text{kg}^{-1}$  in order to maintain consistency with this study and in previous reports, respectively); table S4, maximum observed  $^{137}\text{Cs}$ ,  $^{90}\text{Sr}$ , and  $^{129}\text{I}$  concentrations for all cruises cited in this study (PDF)

## ■ AUTHOR INFORMATION

### Corresponding Author

Jennifer A. Kenyon – Department of Marine Chemistry and Geochemistry, Woods Hole Oceanographic Institution, Woods Hole, Massachusetts 02543, United States; Massachusetts Institute of Technology–Woods Hole Oceanographic Institution Joint Program in Oceanography/Applied Ocean Science and Engineering, Woods Hole, Massachusetts 02543, United States; [orcid.org/0000-0001-6442-2374](https://orcid.org/0000-0001-6442-2374); Phone: +1 508 289 4851; Email: [jkenyon@whoi.edu](mailto:jkenyon@whoi.edu)

### Authors

Ken O. Buesseler – Department of Marine Chemistry and Geochemistry, Woods Hole Oceanographic Institution, Woods Hole, Massachusetts 02543, United States

Núria Casacuberta – Laboratory of Ion Beam Physics, ETH Zurich, 8093 Zurich, Switzerland; [orcid.org/0000-0001-7316-1655](https://orcid.org/0000-0001-7316-1655)

Maxi Castrillejo – Laboratory of Ion Beam Physics, ETH Zurich, 8093 Zurich, Switzerland; [orcid.org/0000-0001-5149-2218](https://orcid.org/0000-0001-5149-2218)

Shigeyoshi Otsuka – Atmosphere and Ocean Research Institute, University of Tokyo, Kashiwa, Chiba 277-8564, Japan; [orcid.org/0000-0003-2087-9676](https://orcid.org/0000-0003-2087-9676)

Pere Masqué – School of Sciences & Centre for Marine Ecosystems Research, Edith Cowan University, Joondalup, WA 6027, Australia; Departament de Física & Institut de Ciència i Tecnologia Ambientals, Universitat Autònoma de Barcelona, Cerdanyola del Valles 08193, Spain

Jessica A. Drysdale – Department of Marine Chemistry and Geochemistry, Woods Hole Oceanographic Institution, Woods

Hole, Massachusetts 02543, United States; [orcid.org/0000-0001-9740-3268](https://orcid.org/0000-0001-9740-3268)

Steven M. Pike – Department of Marine Chemistry and Geochemistry, Woods Hole Oceanographic Institution, Woods Hole, Massachusetts 02543, United States

Virginie Sanial – Université de Toulon, Aix Marseille Université, CNRS/INSU, IRD, MIO UM 110, Mediterranean Institute of Oceanography, UMR7294, 83041 Toulon Cedex 9, France

Complete contact information is available at: <https://pubs.acs.org/10.1021/acs.est.0c05321>

## Author Contributions

The manuscript was written through contributions of all authors. All authors have given approval to the final version of the manuscript.

## Notes

The authors declare no competing financial interest.

Any opinion, findings, and conclusions or recommendations expressed in this material are those of the author(s) and do not necessarily reflect the views of the National Science Foundation.

## ■ ACKNOWLEDGMENTS

This publication was supported the Gordon and Betty Moore Foundation, the Deerbrook Charitable Trust, the EC Seventh Framework Program COMET–FRAME project (grant agreement no. 604974) and the Generalitat de Catalunya (MERS 2017 SGR-1588). This work is contributing to the Institut de Ciència i Tecnologia Ambientals “Unit of Excellence” (MinEco, MDM2015-0552). The authors would like to thank the colleagues, captain, and crew of the R/V Shinsei Maru, and G. Swarr with the WHOI Plasma Mass Spectrometry Facility. The authors would also like to the J. Nishikawa of Tokai University for organizing cruises in 2013 and 2014 (supported by the JSPS KAKENHI, grant number 24110005). This material is based upon work supported by the National Science Foundation Graduate Research Fellowship under Grant No. 1122374. M.C. was supported by FPU PhD studentship AP-2012-2901 from the Ministerio de Educación, Cultura y Deporte of Spain and the ETH Zurich Postdoctoral Fellowship Program (17-2 FEL-30), cofunded by the Marie Curie Actions for People COFUND Program.

## ■ REFERENCES

- (1) Steinhauser, G.; Brandl, A.; Johnson, T. E. Comparison of the Chernobyl and Fukushima nuclear accidents: a review of the environmental impacts. *Sci. Total Environ.* **2014**, *470*, 800–817.
- (2) Buesseler, K. O.; Aoyama, M.; Fukusawa, M. Impacts of the Fukushima nuclear power plants on marine radioactivity. *Environ. Sci. Technol.* **2011**, *45*, 9931–9935.
- (3) Buesseler, K. O.; Dai, M.; Benitez-Nelson, C.; Charmasson, S.; Higley, K.; Maderich, V.; Masqué, P.; Morris, P. J.; Oughton, D.; Smith, J. N. Fukushima Daiichi-Derived Radionuclides in the Ocean: Transport, Fate, and Impacts. *Annu. Rev. Mar. Sci.* **2017**, *9*, 173–203.
- (4) Sanial, V.; Buesseler, K. O.; Charette, M. A.; Nagao, S. Unexpected source of Fukushima-derived radiocesium to the coastal ocean of Japan. *Proc. Natl. Acad. Sci. U. S. A.* **2017**, *41*, 11092–11096.
- (5) Wada, T.; Nemoto, Y.; Shimamura, S.; Fujita, T.; Mizuno, T. Effects of the nuclear disaster on marine products in Fukushima. *J. Environ. Radioact.* **2013**, *124*, 246–254.
- (6) Aoyama, M.; Hirose, K. Artificial radionuclides database in the Pacific Ocean: HAM database. *Sci. World J.* **2004**, *4*, 200–215.

- (7) Ikeuchi, Y. Temporal variations of  $^{90}\text{Sr}$  and  $^{137}\text{Cs}$  concentrations in Japanese coastal surface seawater and sediments from 1974 to 1998. *Deep Sea Res., Part II* **2003**, *50*, 2713–2726.
- (8) Povinec, P. P.; Aarkrog, A.; Buesseler, K. O.; Delfanti, R.; Hirose, K.; Hong, G. H.; Ito, T.; Livingston, H. D.; Nies, H.; Noshkin, V. E.; Shima, S.; Togawa, O.  $^{90}\text{Sr}$ ,  $^{137}\text{Cs}$ , and  $^{239,240}\text{Pu}$  concentrations surface water time series in the Pacific and Indian Oceans – WOMARS results. *J. Environ. Radioact.* **2005**, *81*, 63–87.
- (9) Guilderson, T. P.; Tumej, S. J.; Brown, T. A.; Buesseler, K. O. The 129-iodine content of subtropical Pacific waters: impact of Fukushima and other anthropogenic 129-I sources. *Biogeosciences* **2014**, *11*, 4839–4852.
- (10) Suzuki, T.; Otsuka, S.; Kuwabara, J.; Kawamura, H.; Kobayashi, T. Iodine-129 concentration in seawater near Fukushima before and after the accident at the Fukushima Daiichi Nuclear Power Plant. *Biogeosciences* **2013**, *10*, 3839–3847.
- (11) Aoyama, M.; Kajino, M.; Tanaka, T. Y.; Sekiyama, T. T.; Tsumune, D.; Tsubono, T.; Hamajima, Y.; Inomata, Y.; Gamo, T.  $^{134}\text{Cs}$  and  $^{137}\text{Cs}$  in the North Pacific Ocean derived from the March 2011 TEPCO Fukushima Dai-ichi Nuclear Power Plant accident, Japan. Part two: estimation of  $^{134}\text{Cs}$  and  $^{137}\text{Cs}$  inventories in the North Pacific. *J. Oceanogr.* **2016**, *72*. DOI: 10.1007/s10872-015-0332-2.
- (12) Casacuberta, N.; Masqué, P.; Garcia-Orellana, J.; Garcia-Tenorio, R.; Buesseler, K. O.  $^{90}\text{Sr}$  and  $^{89}\text{Sr}$  in seawater off Japan as a consequence of the Fukushima Dai-ichi nuclear accident. *Biogeosciences* **2013**, *10*, 3649–3659.
- (13) Povinec, P. P.; Hirose, K.; Aoyama, M. Radiostrontium in the western North Pacific: Characteristics, Behavior, and the Fukushima impact. *Environ. Sci. Technol.* **2012**, *46*, 10356–10363.
- (14) Tanaka, K.; Shimada, A.; Hoshi, A.; Yasuda, M.; Ozawa, M.; Kameo, Y. Radiochemical analysis of rubble and trees collected from the Fukushima Daiichi nuclear power station. *J. Nucl. Sci. Technol.* **2014**, *51*, 1032–1043.
- (15) Japan Atomic Energy Agency (JAEA). Database for Radioactive Substance Monitoring Data; [embd.jaea.go.jp](http://embd.jaea.go.jp) (accessed November 2017).
- (16) Castrillejo, M.; Casacuberta, N.; Breier, C. F.; Pike, S. M.; Masqué, P.; Buesseler, K. O. Reassessment of  $^{90}\text{Sr}$ ,  $^{137}\text{Cs}$ , and  $^{134}\text{Cs}$  in the Coast off Japan Derived from the Fukushima Dai-ichi Nuclear Accident. *Environ. Sci. Technol.* **2016**, *50*, 173–180.
- (17) Hou, X.; Povinec, P. P.; Zhang, L.; Shi, K.; Biddulph, D.; Chang, C.; Fan, Y.; Golser, R.; Hou, Y.; Jeskovsky, M.; Tim Jull, A. J.; Liu, Q.; Luo, M.; Steier, P.; Zhou, W. Iodine-129 in Seawater Offshore Fukushima: Distribution, Inorganic Speciation, Sources, and Budget. *Environ. Sci. Technol.* **2013**, *47*, 3091–3098.
- (18) Casacuberta, N.; Christl, M.; Vockenhuber, C. *Chemistry of 129I in seawater samples: setting up the 129I radiochemistry at LIP/EAWAG*; ETH: Zurich, 2014, 140.
- (19) Miyake, Y.; Matsuzaki, H.; Fujiwara, T.; Saito, T.; Yamagata, T.; Honda, M.; Muramatsu, Y. Isotopic ratio of radioactive iodine  $^{129}\text{I}/^{131}\text{I}$  released from the Fukushima Daiichi NPP accident. *Geochem. J.* **2012**, *46* (4), 327–333.
- (20) Snyder, G.; Aldahan, A.; Possnert, G. Global distribution and long-term fate of anthropogenic  $^{129}\text{I}$  in marine and surface water reservoirs. *Geochem., Geophys., Geosyst.* **2010**, *11*, Q04010.
- (21) Smith, J. N.; McLaughlin, F. A.; Smethie, W. M.; Moran, S. B.; Lepore, K. Iodine-129,  $^{137}\text{Cs}$ , and CFC-11 tracer transit time distributions in the Arctic Ocean. *J. Geophys. Res.* **2011**, *116*, C04024.
- (22) Tsumune, D.; Tsubono, T.; Aoyama, M.; Uematsu, M.; Misumi, K.; Maeda, Y.; Yoshida, Y.; Hayami, H. One-year, regional-scale simulation of  $^{137}\text{Cs}$  radioactivity in the ocean following the Fukushima Dai-ichi Nuclear Power Plant accident. *Biogeosciences* **2013**, *10*, 5601–5617.
- (23) Casacuberta, N.; Christl, M.; Buesseler, K. O.; Lau, Y.; Vockenhuber, C.; Castrillejo, M.; Synal, H.; Masqué, P. Potential Releases of  $^{129}\text{I}$ ,  $^{236}\text{U}$ , and Pu Isotopes from the Fukushima Dai-ichi Nuclear Power Plants to the Ocean from 2013 to 2015. *Environ. Sci. Technol.* **2017**, *51*, 9826–9835.
- (24) Buesseler, K. RiOSMethod:  $^{137}\text{Cesium}$  Column Chemistry—20 L Seawater Samples. *RiOS Cookbook* (<https://cmer.whoi.edu/recipe/cs-from-20l-using-knifc-pan-resin/>). 2013.
- (25) Šebesta, F. Composite sorbents of inorganic ion-exchangers and polyacrylonitrile binding matrix. *J. Radioanal. Nucl. Chem.* **1997**, *220* (1), 77–88.
- (26) Breier, C. F.; Pike, S. M.; Šebesta, F.; Tradd, K.; Breier, J. A.; Buesseler, K. O. New applications of KNiFC-PAN resin for broad scale monitoring of radiocesium following the Fukushima Dai-ichi nuclear disaster. *J. Radioanal. Nucl. Chem.* **2016**, *307*, 2193–2200.
- (27) Casacuberta, N.; Masqué, P.; Garcia-Orellana, J.; Lopez-Castillo, E.; Kenna, T. C.; Garcia-Tenorio, R. A sequential method for the determination of  $^{90}\text{Sr}$ , Pu- isotopes and  $^{137}\text{Cs}$  in seawater. *Biogeosciences* **2013**, *10*, 3649–3659.
- (28) Tazoe, H.; Obata, H.; Tomita, M.; Namura, S.; Nishioka, J.; Yamagata, T.; Karube, Z.; Yamada, M. Novel method for low level Sr-90 activity detection in seawater by combining oxalate precipitation and chelating resin extraction. *Geochem. J.* **2017**, *50*, 193–197.
- (29) Christl, M.; Vockenhuber, C.; Kubik, P. W.; Wacker, L.; Lachner, J.; Alifimov, V.; Synal, H. A. The ETH Zurich AMS facilities: Performance parameters and reference materials. *Nucl. Instrum. Methods Phys. Res., Sect. B* **2013**, *294* (0), 29–38.
- (30) Michel, R.; Daraoui, A.; Gorny, M.; Jakob, D.; Sachse, R.; Tosch, L.; Nies, H.; Goroncy, I.; Herrmann, J.; Synal, H. A.; Stocker, M.; Alifimov, V. Iodine-129 and iodine-127 in European seawaters and in precipitation from Northern Germany. *Sci. Total Environ.* **2012**, *419*, 151–169.
- (31) Schlitzer, R., Ocean Data View, <http://odv.awi.de>, 2016.
- (32) Otsuka, S.; Satoh, Y.; Suzuki, T.; Kuwabara, J.; Nakanishi, T. Distribution and fate of  $^{129}\text{I}$  in the seabed sediment off Fukushima. *J. Environ. Radioact.* **2018**, *192*, 208–218.
- (33) Nakamura, Y. Studies on the fishing ground formation of Sakhalin surf clam and the hydraulic environment in coastal region. *Fukushima suisan shikenjo Res. Rep.* **1991**, 1–118.
- (34) Casacuberta, N. Personal communication of currently unpublished data and findings, November 15, 2019.
- (35) Rypina, I. I.; Jayne, S. R.; Yoshida, S.; Macdonald, A. M.; Douglass, E.; Buesseler, K. O. Short-term dispersal of Fukushima-derived radionuclides off Japan: modeling efforts and model-data intercomparison. *Biogeosciences* **2013**, *10*, 4973–4990.
- (36) Maderich, V.; Bezhenar, R.; Heling, R.; de With, G.; Jung, K. T.; Myoung, J. G.; Cho, Y. K.; Qiao, F.; Robertson, L. Regional long-term model of radioactivity dispersion and fate in the Northwestern Pacific and adjacent seas: application to the Fukushima Dai-ichi accident. *J. Environ. Radioact.* **2014**, *131*, 4–18.
- (37) Tumej, S. J.; Guilderson, T. P.; Brown, T. A.; Buesseler, K. O. Input of  $^{129}\text{I}$  into the western Pacific Ocean resulting from the Fukushima nuclear event. *J. Radioanal. Nucl. Chem.* **2013**, *296*, 957–962.
- (38) Japan Meteorological Agency. History of daily weather observations at Station Namie, Fukushima Prefecture, Japan. <https://www.jma.go.jp/jma/> (accessed March 2018).
- (39) Chartin, C.; Evrard, O.; Onda, Y.; Patin, J.; Lefevre, I.; Ottele, C.; Ayrault, S.; Lepage, H.; Bonte, P. Tracking the early dispersion of contaminated sediment along rivers draining the Fukushima radioactive pollution plume. *Anthropocene* **2013**, *1*, 23–24.
- (40) Nagao, S.; Kanamori, M.; Ochiai, S.; Tomihara, S.; Fukushi, K.; Yamamoto, M. Export of  $^{134}\text{Cs}$  and  $^{137}\text{Cs}$  in the Fukushima river systems at heavy rains by Typhoon Roke in September 2011. *Biogeosciences* **2013**, *10*, 6215–6223.
- (41) Evrard, O.; Lacey, J. P.; Lepage, H.; Onda, Y.; Cerdan, O.; Ayrault, S. Radiocesium transfer from hillslopes to the Pacific Ocean after the Fukushima nuclear power plant accident: a review. *J. Environ. Radioact.* **2015**, *148*, 92–110.
- (42) Takata, H.; Hasegawa, K.; Oikawa, S.; Kudo, N.; Ikenoue, T.; Isono, R. S.; Kusakabe, M. Remobilization of radiocesium on riverine particles in seawater: the contribution of desorption to the export flux to the marine environment. *Mar. Chem.* **2015**, *176*, 51–63.

(43) Kakehi, S.; Kaeriyama, H.; Ambe, D.; Ono, T.; Ito, S.; Shimizu, Y.; Watanabe, T. Radioactive cesium dynamics derived from hydrographic observations in the Abukuma River Estuary, Japan. *J. Environ. Radioact.* **2016**, *153*, 1–9.

(44) Tokyo Electric Power Company (TEPCO). Overflow of rainwater from “Drainage K” into the sea due to heavy rainfall. 2015. [http://www.tepco.co.jp/en/nu/fukushima-np/handouts/2015/images/handouts\\_150716\\_01-e.pdf](http://www.tepco.co.jp/en/nu/fukushima-np/handouts/2015/images/handouts_150716_01-e.pdf) (accessed November 2017).

(45) Tokyo Electric Power Company (TEPCO). Contaminated Water Treatment. [https://www7.tepco.co.jp/responsibility/decommissioning/action/w\\_management/treatment-e.html](https://www7.tepco.co.jp/responsibility/decommissioning/action/w_management/treatment-e.html) (accessed November 2019).

(46) BBC. Fukushima: Radioactive water may be dumped in Pacific. <https://www.bbc.com/news/world-south-asia-49649687> (accessed October 2019).

(47) Ministry of Economy, Trade, and Industry (METI). The Outline of the Handling of ALPS Treated Water at Fukushima Daiichi NPS (FDNPS). [https://www.meti.go.jp/english/earthquake/nuclear/decommissioning/pdf/20191121\\_current\\_status.pdf](https://www.meti.go.jp/english/earthquake/nuclear/decommissioning/pdf/20191121_current_status.pdf) (accessed November 2019).

(48) Buessler, K. O. Opening the floodgates at Fukushima: Tritium is not the only radioisotope of concern for stored contaminated water. *Science* **2020**, *369* (6504), 621–622.